Collective Motion

Dylan Scott

Durham University, Department of Physics

In this paper, I investigate the nature of collective motion by studying and recreating more and more complex models and making observations about fundamental parameters. In the single species models I measure the instability and transition into disordered motion that occurs as the magnitude of the randomness in the movement is increased. Later, with the two species models that focus on predator and prey type systems, I investigate the lifetime of the prey species as I tweak around the fundamental starting parameters for each system.

CONTENTS

1. INTRODUCTION

The concept of collective motion covers a wide range of behaviours observed in nature. These behaviours include the coordinated flocking of birds, the fluid-like movements of schools of fish, the swarming of insects, and other such behaviours. It also includes the sudden disruption of such patterns, reducing the ordered structure of a flock of starlings into a chaotic fluttering mess in the presence of a predatory species, for example. Overall, collective motion can be considered as the coordination of a large group due to very simple rules followed by each individual.

As a research field, it has been discovered that collective motion may be applied in areas outside of ecological systems. Certain physical and chemical systems contain the presence of "self-propelled particles" which may act in similar nature to the macroscopic animals described previously. For example, recent studies have examined things such as water condensation droplets [1] and fermionic gases [2]. Given the vast amount of diverse situations in which the fundamental principles of collective motion apply, it is of interest that this field be studied. Grasping the underlying concepts may allow for a better understanding of physical and chemical systems, and could also pave the way for future technological advancements. At present, there have already been many studies investigating the applications of collective motion in autonomous drone flocks [3–5]. These studies highlight the potential for practical implementations, where machines are capable of mirroring the coordination and collective behaviours observed in various ecosystems.

As interesting as it would be to explore possible avenues for practical applications, the goal of this report will be to provide an exploration of the concept of collective motion. I will cover the details of collective motion as described in other research papers and articles and in addition will also be including my findings in the subject. I will review several models constructed from previous reports and articles, recreate, and then test them.
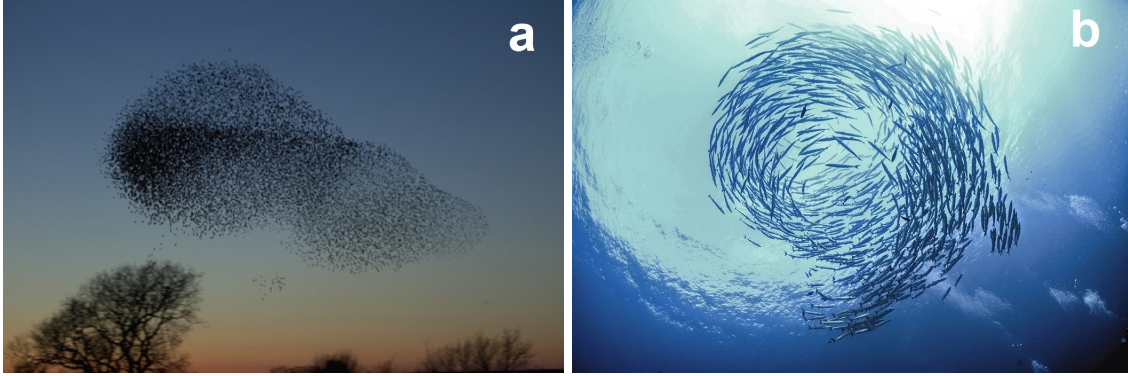
FIG. 1: A couple examples showcasing the complex collective motions that can be observed in nature. (a) a flock of birds (b) a vortex of schooling fish.

1.1. Basics of collective motion

Collective motion is the name for the appearance of coherent behaviours or ordered movements from a group of individual units. The underlying principle is that each body may only follow a few simple rules, but this can result in the group performing a range of complex movements. In general, collective motion normally occurs within a system when the units follow simple baseline rules:

- They are rather similar

- Move with near constant absolute velocity whilst capable of changing direction

- Interact within a specific interaction range and change direction based on its surrounding units

- Are subject to a noise of varying magnitude when choosing their movement direction

These rules, as specified by Vicsek [6], govern the base principles that apply to all systems exhibiting collective motion.

In nature, more complex motions and behaviours may arise as seen in Fig. 1. The cause for such movements may be due to benefits to the species, such as protection from predators, or better efficiency in conserving stamina.
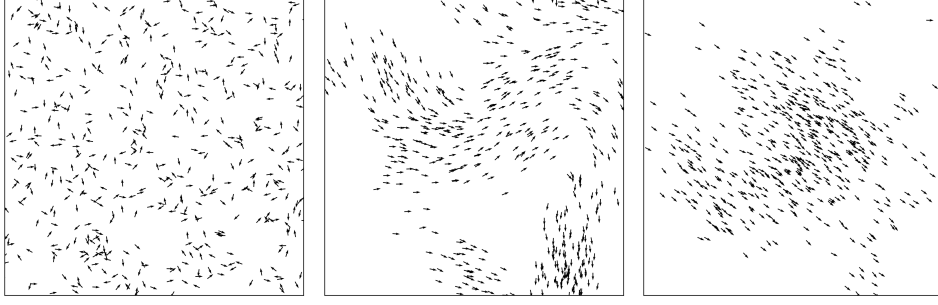
FIG. 2: The evolution of the Vicsek model over time. The agents start out moving in random directions but quickly align themselves with each other.

2. VICSEK MODEL

One of the first papers published on the subject was by Vicsek et al [7]. Their paper focused on the complex cooperative behaviours that could be seen in particle systems going through a phase transition. They came up with a simple model to replicate this behaviour.

2.1. Vicsek Model Setup

A set of N particles are placed within a 2D box of length L with periodic bounds. Initially, each particle has a random starting position $\mathbf{x}_i(t)$ and is set to move in a random direction $\theta_i(t)$. The velocity $\mathbf{v}_i(t)$ of each particle is set to a constant speed $|\mathbf{v}_i(t)| = v$. After every timestep Δt in the simulation, the positions and direction angles of the particles are adjusted in the following way:

$$\mathbf{x}_i(t + \Delta t) = \mathbf{x}_i(t) + \mathbf{v}_i(t) \cdot \Delta t \tag{1}$$

$$\theta_i(t + \Delta t) = \langle \theta(t) \rangle_R + \Delta \theta \tag{2}$$

The positions of the particles are updated in the usual way. The direction angle of each particle is calculated by taking the average angle of all neighbouring particles within an interaction radius R and adding a $\Delta \theta$ term which corresponds to a random perturbation of the angle. The average angle may be calculated by

$$\langle \theta(t) \rangle_R = \tan^{-1} \left(\frac{\langle \sin(\theta) \rangle_R}{\langle \cos(\theta) \rangle_R} \right) . \tag{3}$$

In their paper, Vicsek et al used a uniform distribution to choose the $\Delta \theta$ for each particle, at each timestep. They chose a random value from the range $[-\eta/2, \eta/2]$ to perturb the direction of the
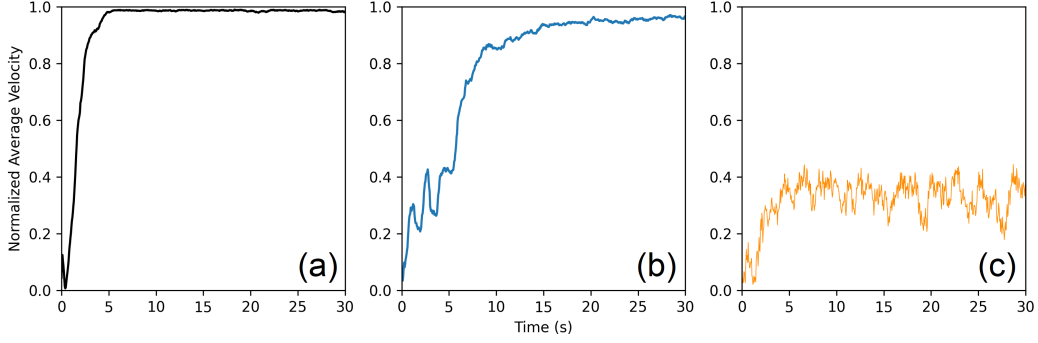
FIG. 3: The behaviour of the normalized average velocity φ with time. (a) The base case $N = 500, R = 1, \eta = 0.5$. (b) Smaller interaction radius $R = 0.3$. (c) Greater magnitude for the noise parameter $\eta = 4$.

particle, which represents the noise of the system. The magnitude of the noise may be controlled by adjusting the η parameter. In their paper, an order parameter $\varphi(t)$ was introduced to measure the alignment of the trajectories of the particles. It represents the normalized average velocity of the particles and may be calculated by

$$\varphi(t) = \frac{1}{Nv} \left| \sum_{i=1}^{N} \mathbf{v}_i(t) \right| . \tag{4}$$

φ therefore has a range between 0 (completely disordered motion) and 1 (fully aligned motion). The paper then goes on to inspect the effects of the various system parameters on this order parameter. The parameters that can be changed are the number of particles N, the interaction radius R for aligning with neighbouring particles, and the strength of the noise η.

2.2. Vicsek Model Results

I have produced an investigation into this model and the effects of the various parameters on the order parameter φ. The results can be seen in Fig. 3 and Fig. 4. Initially I used the same parameters as in the Vicsek paper and measured φ over a period of 30 seconds, which can be seen in Fig. 3a. The value quickly approached 1 and stayed there for the rest of the simulation. I then reduced the size of the interaction radius R to 30% its initial size. The result is that φ took longer to tend towards the previous value of 1. Intuitively, this makes sense as fewer interactions between particles would imply taking a longer time to self-align with each other. Next, I returned R back to its initial value and increased the noise magnitude η eightfold from $\eta = 0.5$ to 4. This had the
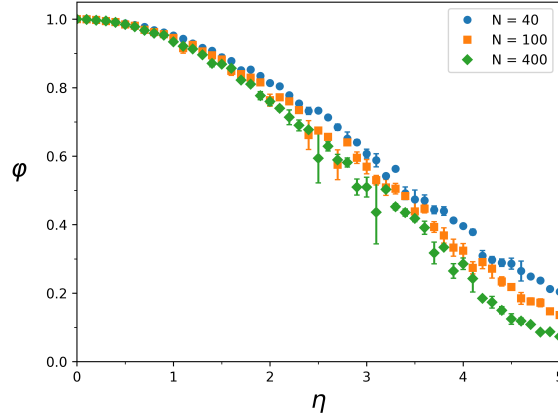
FIG. 4: The average value of φ after $t = 300$ seconds, for varying noise magnitude η and particle number N.

effect of reducing the value that φ tended towards, as well as cause instability in the value as it jumped up and down. It would be interesting to investigate the size of this fluctuation in a later study but at the time I was only interested in the value the average tended towards as this is what was conducted in the paper by Vicsek et al.

Fig. 4 is the data I received after measuring the average value of φ for various noise magnitudes η and particle numbers N. The figure itself visually matches a similar figure produced in the paper [7], which measured the same parameters with the same conditions. I can therefore say I have successfully reproduced their results and can make similar conclusions. In the paper they note that the order parameter φ is similar to an order parameter for some equilibrium systems close to their melting point.

3. CHASE & ESCAPE MODEL

Whilst the previous model was interesting, I preferred to investigate systems that are more natural and less abstract. I also was interested in studying areas in collective motion that aren't investigated as often. For these reasons I decided to look into two species systems, where one species' goal is to hunt the other. This type of system appears very frequently in nature, with groups of predators hunting down herds of prey.

When focusing on this area, I encountered a paper authored by Janosov, with Vicsek et al as co-authors [8]. In this paper, they discuss a system in which a group of 'chasers' are trying to

catch another group of 'escapers'. The chasers aren't as fast as the escapers so they need to use cooperative behaviours and smart tactics to successfully catch the escapers. Instead of using fixed velocities, there are now simulated 'forces' which can accelerate the individual species agents up to a maximum top speed.

3.1.   Chase & Escape Model Setup

There are now N_c chasers and N_e escapers in a system, with top speeds $v_{max,c}$ and $v_{max,e}$ but a similar top acceleration a_{max}. The position and velocity of the ith chaser are denoted by $\mathbf{x}_{c,i}$ and $\mathbf{v}_{c,i}$ respectively. Similarly, $\mathbf{x}_{e,j}$ and $\mathbf{v}_{e,j}$ denote the position and velocity of the jth escaper. An escaper is 'caught' if the distance between it and the closest chaser decreases below a specified capture distance r_{cd}. The simulation will end once all escapers are caught.

3.1.1.   General rules

The first difference to the previous model is that the system now takes place within a finite circular field of radius r_a, with the origin of our coordinate space at the center. The author of the paper stated that this was chosen to remove edge-effects as much as possible. The field itself is surrounded by a soft wall [9] which repulses the species towards the center:

$$\mathbf{v}_i^a = s(x_i, r_a, r_{wall}) \cdot \left(v_{max,k} \frac{\mathbf{x}_i}{x_i} + \mathbf{v}_i \right), \quad (k = c, e) \tag{5}$$

where

$$s(x_i, r_a, r_{wall}) = \begin{cases} 0 & \text{if } x_i \leq r_a \\ -\sin^2\left(\frac{\pi}{2\,r_{wall}}(x_i - r_a) \right) & \text{if } r_a \leq x_i \leq r_a + r_{wall} \\ -1 & \text{if } x_i \geq r_a + r_{wall} \end{cases} \tag{6}$$

with r_{wall} the width of the soft wall and $x_i = |\mathbf{x}_i|$.

Within each species there is also a repulsive force applied between the individual units in order to prevent collisions:

$$v_{k,i}^{coll} = v_{max,k}\,\hat{\mathcal{N}} \left[\sum_{j=1}^{N_k} \frac{r_{cd} - d_{ij}}{d_{ij}}\, \mathbf{d}_{ij}\, \Theta(r_{cd} - d_{ij}) \right] \tag{7}$$

$$\mathbf{d}_{ij} = \mathbf{x}_{k,i} - \mathbf{x}_{k,j}, \quad d_{ij} = |\mathbf{d}_{ij}| \quad (k = c, e) \tag{8}$$

where Θ is the Heaviside step function and $\hat{\mathcal{N}}$ is a vector normalization operator.

3.1.2. Chasers

Chasers will chase the closest escaper whilst working together with other chasers to encircle their prey. The chasing force is attractive between the chaser and its target and is given by

$$\mathbf{v}_{c,i}^{ch} = v_{max,c}\,\hat{\mathcal{N}}\left[\frac{\mathbf{x}_e - \mathbf{x}_{c,i}}{|\mathbf{x}_e - \mathbf{x}_{c,i}|} + C_f'\frac{\mathbf{v}_e - \mathbf{v}_{c,i}}{|\mathbf{v}_e - \mathbf{v}_{c,i}|^2}\right] \tag{9}$$

where C_f' is the coefficient for a velocity alignment term which takes precedence at small distances.

Chasers also try to predict the path of the escapers and intercept them. Instead of aiming for the target position $\mathbf{x}_e$ they instead head towards the point $\mathbf{x}_e' = \mathbf{x}_e + \mathbf{v}_e \cdot \tau_{pred}$ which lies along the current trajectory of the escaper. τ_{pred} is how far into the future the chaser will predict the escaper to continue on its trajectory. If the chaser can intercept the escaper along its trajectory before this point, it should instead head to the interception point. $\mathbf{x}_e'$ is therefore the solution to the equation

$$\mathbf{x}_e' = \mathbf{x}_e + \mathbf{v}_e \cdot \min\left[\frac{\mathbf{x}_e' - \mathbf{x}_c}{|\mathbf{v}_c|}, \tau_{pred}\right]. \tag{10}$$

Finally, chasers have an interaction force applied between them. This is to simulate cooperative behaviour. If there was no cooperation, the chasers will all lag behind the escapers with no chance of catching them. Janosov et al modelled this as a repulsive force between the chasers in order to keep them spread out:

$$\mathbf{v}_{c,i}^{inter} = C_{inter}\,v_{max,c}\,\hat{\mathcal{N}}\left[\sum_j\left(\frac{r_{inter} - d_{ij}}{d_{ij}}\mathbf{d}_{ij} + C_f''\frac{\mathbf{v}_{c,j} - \mathbf{v}_{c,i}}{d_{ij}^2}\right)\right] \tag{11}$$

$$\mathbf{d}_{ij} = \mathbf{x}_{c,i} - \mathbf{x}_{c,j}, \qquad d_{ij} = |\mathbf{d}_{ij}| \tag{12}$$

where r_{inter} is the characteristic length of this repulsion whilst C_f'' is the coefficient of a velocity alignment term.

The final force on the ith chaser is the sum of the general and chaser specific terms

$$\mathbf{f}_{c,i} = \mathbf{v}_i^a + \mathbf{v}_{c,i}^{coll} + \mathbf{v}_{c,i}^{ch} + \mathbf{v}_{c,i}^{inter} \tag{13}$$

3.1.3. Escapers

For the model in the paper, each escaper has a radius r_{sense} around them in which they can detect any chasers. When an escaper detects chasers around them, there will be a repulsive force between each chaser and the escaper applied to the escaper proportional to the inverse squared distance

between. This represents a prey species prioritising closer predators when choosing which direction to escape. The term is given by

$$\mathbf{v}_{e,i}^{esc} = v_{max,e}\,\hat{\mathcal{N}}\left[\sum_j \left(\frac{\mathbf{x}_{e,i} - \mathbf{x}_{c,j}}{|\mathbf{x}_{e,i} - \mathbf{x}_{c,j}|^2} - C_f''' \frac{\mathbf{v}_{e,i} - \mathbf{v}_{c,j}}{|\mathbf{x}_{e,i} - \mathbf{x}_{c,j}|^2}\right)\Theta(r_{sense} - |\mathbf{x}_{e,i} - \mathbf{x}_{c,j}|)\right]. \qquad (14)$$

This form of escaping alone is quite simple and basic. Janosov introduced erratic escaping into their as a means to replicate the erratic movements a prey species might make whilst fleeing for its life. They introduce zigzagging into the escapers' behaviour as a way to represent more realistic behaviours seen in nature. Each escaper has a panic parameter p_{panic} which is an exponential function of the minimum distance to the closet chaser d_{min}. It is calculated by

$$p_{panic} = \begin{cases} \frac{1}{e-1}\left[e^{1-d_{min}/r_{sense}} - 1\right] & d_{min} \leq r_{sense} \\ 0 & d_{min} \geq r_{sense} \end{cases} \qquad (15)$$

therefore p_{panic} ranges from 0 when it does not detect any chasers to 1 when the closest chaser is at the same position as the escaper. Once the panic parameter meets the threshold $p_{panic} > p_{thresh}$, and assuming there's at least a reasonable distance r_{zigzag} from the wall ($r_a - |\mathbf{x}_e| > r_{zigzag}$) the escaper will begin zigzagging in order to avoid its pursuers. The direction angle is chosen randomly from the range $[0, 2\pi]$ and the magnitude of the zigzag component $|\mathbf{v}_{e,i}^{zigzag}| = v_{max,e}$. The length of time spent on a single zigzag length is also a random parameter with a lower bound $r_{zigzag}/v_{max,e}$ and upper bound $r_a/v_{max,e}$.

To account for possibly of an escaper trying to flee outside the wall and reducing its speed as a result, Janosov adds a condition where the radial part of the velocity decreases the closer to the wall the escaper gets.

$$\mathbf{v}_e^{final} = \mathbf{v}_e - C_{wall}\frac{\mathbf{x}_e}{|\mathbf{x}_e|}\left(\frac{\mathbf{x}_e}{|\mathbf{x}_e|}\cdot\mathbf{v}_e\right) = \hat{\mathbf{W}}\mathbf{v}_e \qquad (16)$$

where

$$C_{wall} = \begin{cases} 1 & r_a - |\mathbf{x}_e| < 2\,r_{wall} \\ \cos^2\left(\frac{\pi}{2\,r_{zigzag}}(|\mathbf{x}_e| - r_a + 2r_{wall})\right) & r_a - |\mathbf{x}_e| < 2\,r_{wall} + r_{zigzag} \\ 0 & \text{otherwise.} \end{cases} \qquad (17)$$

By itself, this would cause the escaper to get stuck at the wall once it reaches there. A condition is therefore introduced: if the escaper is close to wall ($C_{wall} > 0.5$) and it is capable of slipping
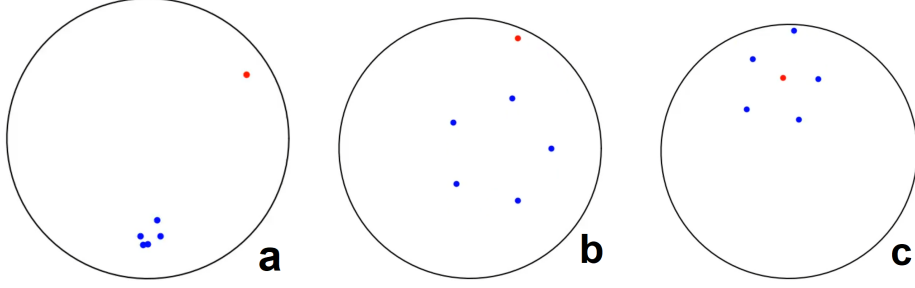
FIG. 5: The time evolution of the chase & escape model. The chasers (blue) hunt down the escaper (red) and encircle it before quickly catching it.

past the two closest chasers and return to the center of the field, it will do so. To calculate if it is possible, first determine the direction vector pointing along the line which evenly separates the two chasers

$$\mathbf{e} = \frac{(\mathbf{x}_{c,1} - \mathbf{x}_e) + (\mathbf{x}_{c,2} - \mathbf{x}_e)}{|(\mathbf{x}_{c,1} - \mathbf{x}_e) + (\mathbf{x}_{c,2} - \mathbf{x}_e)|} . \tag{18}$$

Then calculate the two points at which the two chasers will perpendicularly bisect the line

$$\mathbf{x}_{p,k} = \mathbf{x}_e + \mathbf{e}\left[\mathbf{e} \cdot (\mathbf{x}_{c,k} - \mathbf{x}_e)\right] \quad (k = 1, 2). \tag{19}$$

The minimum times for the escaper to reach those points are given by

$$\tau_{e,k} = \frac{|\mathbf{x}_{p,k} - \mathbf{x}_e|}{v_{max,e}} \tag{20}$$

whilst the times for the chasers are

$$\tau_{c,k} = \frac{|\mathbf{x}_{p,k} - \mathbf{x}_{c,k}| - r_{cd}}{v_{max,c}} . \tag{21}$$

If $\tau_{e,k} < \tau_{c,k}$ for both $k = 1$ and 2, the escaper can successfully pass between the two chasers and return to the center. Otherwise, it stays at the wall.

The final force on the ith escaper is the sum of the general terms and either the basic escaping force or the zigzag force, transformed by the $\hat{\mathbf{W}}$ operator in Eq. 16.

$$\mathbf{f}_{e,i} = \hat{\mathbf{W}}(\mathbf{v}_i^a + \mathbf{v}_{e,i}^{coll} + (\mathbf{v}_{e,i}^{esc} \text{ or } \mathbf{v}_{e,i}^{zigzag})) \tag{22}$$

3.2. Chase & Escape Model Results

[1] M. Lin, P. Kim, S. Arunachalam, R. Hardian, S. Adera, J. Aizenberg, X. Yao, and D. Daniel, Emergent collective motion of self-propelled condensate droplets, arXiv preprint arXiv:2311.06775 (2023).

[2] R. R. Wang and J. L. Bohn, Viscous damping in weltering motion of trapped hydrodynamic dipolar fermi gases, arXiv preprint arXiv:2306.00250 (2023).

[3] M. Verdoucq, G. Theraulaz, R. Escobedo, C. Sire, and G. Hattenberger, Bio-inspired control for collective motion in swarms of drones, in *2022 International Conference on Unmanned Aircraft Systems (ICUAS)* (IEEE, 2022) pp. 1626–1631.

[4] H. Zhao, H. Liu, Y.-W. Leung, and X. Chu, Self-adaptive collective motion of swarm robots, IEEE Transactions on Automation Science and Engineering **15**, 1533 (2018).

[5] D. Albani, T. Manoni, M. Saska, and E. Ferrante, Distributed three dimensional flocking of autonomous drones, in *2022 International Conference on Robotics and Automation (ICRA)* (IEEE, 2022) pp. 6904–6911.

[6] T. Vicsek and A. Zafeiris, Collective motion, Physics reports **517**, 71 (2012).

[7] T. Vicsek, A. Czirók, E. Ben-Jacob, I. Cohen, and O. Shochet, Novel type of phase transition in a system of self-driven particles, Physical review letters **75**, 1226 (1995).

[8] M. Janosov, C. Virágh, G. Vásárhelyi, and T. Vicsek, Group chasing tactics: how to catch a faster prey, New Journal of Physics **19**, 053003 (2017).

[9] J. Han, M. Li, and L. Guo, Soft control on collective behavior of a group of autonomous agents by a shill agent, Journal of Systems Science and Complexity **19**, 54 (2006).

SCIENTIFIC SUMMARY FOR GENERAL AUDIENCE

Collective motion is the name for the cooperative behaviour that can be observed in nature. From a flock of starlings flowing together like water, to a school of fish milling in a vortex, and even the movement of microorganisms, the phenomenon of collective motion can be observed. But why do these species move in such a complex and ordered way? What is the benefit? The goal of this paper is to analyse such systems, by recreating the scientific models of previous researchers and building up an understanding of the nature of collective motion.